

GaussVideoDreamer: 3D Scene Generation with Video Diffusion and Inconsistency-Aware Gaussian Splatting

Junlin Hao
Peking University
Beijing, China
junlin.hao@stu.pku.edu.cn

Peiheng Wang
Peking University
Beijing, China
peiheng.wang@pku.edu.cn

Haoyang Wang
Peking University
Beijing, China
haoyang.wang@stu.pku.edu.cn

Xinggong Zhang
Peking University
Beijing, China
zhangxg@pku.edu.cn

Zongming Guo
Peking University
Beijing, China
guozongming@pku.edu.cn

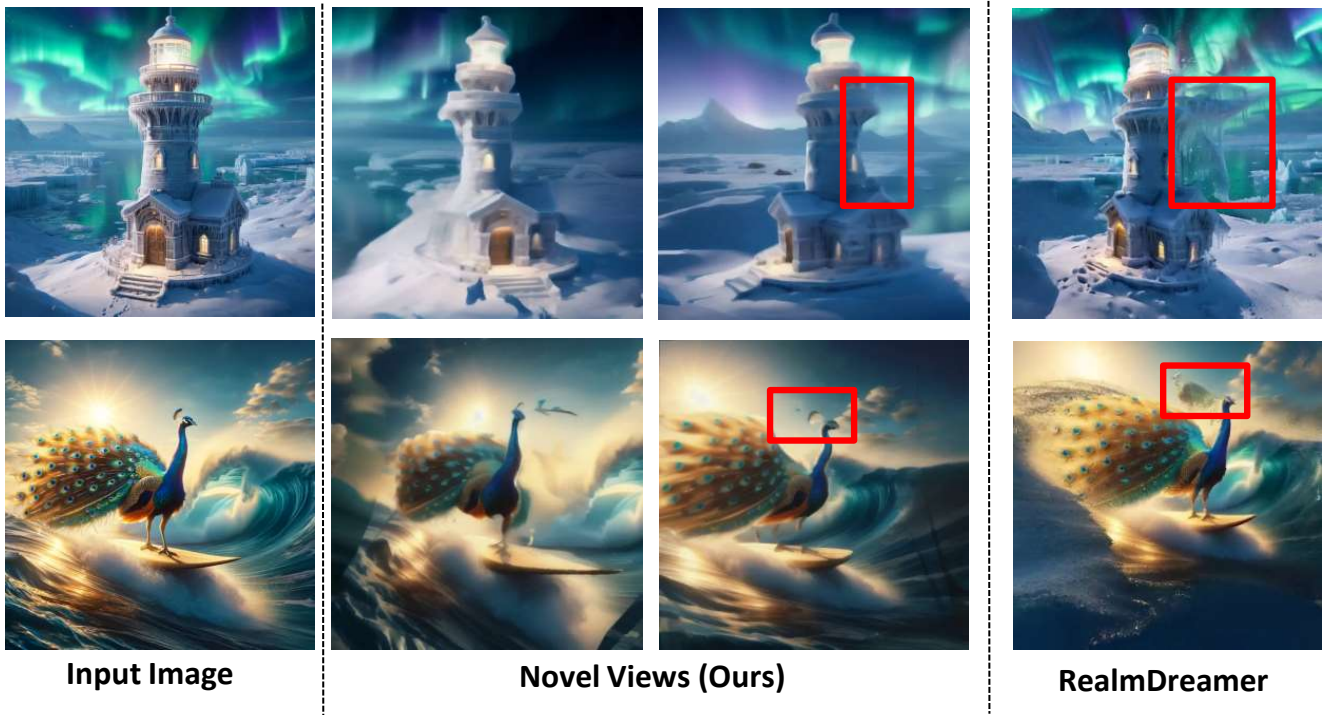


Figure 1: Given a single input image, GaussVideoDreamer generates high-quality 3D scenes with faster processing and improved scene context understanding compared to our baselines [46], especially in the occluded and background regions.

Abstract

Single-image 3D scene reconstruction presents significant challenges due to its inherently ill-posed nature and limited input

constraints. Recent advances have explored two promising directions: **multiview generative models** that train on 3D consistent datasets but struggle with out-of-distribution generalization, and **3D scene inpainting and completion** frameworks that suffer from cross-view inconsistency and suboptimal error handling, as they depend exclusively on depth data or 3D smoothness, which ultimately degrades output quality and computational performance. Building upon these approaches, we present **GaussVideoDreamer**, which advances generative multimedia approaches by bridging the gap between image, video, and 3D generation, integrating their strengths through two key innovations: (1) A progressive video inpainting strategy that harnesses temporal coherence for improved multiview consistency and faster convergence. (2) A 3D Gaussian

Permission to make digital or hard copies of all or part of this work for personal or classroom use is granted without fee provided that copies are not made or distributed for profit or commercial advantage and that copies bear this notice and the full citation on the first page. Copyrights for components of this work owned by others than the author(s) must be honored. Abstracting with credit is permitted. To copy otherwise, or republish, to post on servers or to redistribute to lists, requires prior specific permission and/or a fee. Request permissions from permissions@acm.org.
ACM MM '25, Dublin, Ireland

© 2025 Copyright held by the owner/author(s). Publication rights licensed to ACM.
ACM ISBN 978-1-4503-XXXX-X/2018/06
<https://doi.org/XXXXXXXX.XXXXXXX>

Splatting consistency mask to guide the video diffusion with 3D consistent multiview evidence. Our pipeline combines three core components: a geometry-aware initialization protocol, Inconsistency-Aware Gaussian Splatting, and a progressive video inpainting strategy. Experimental results demonstrate that our approach achieves 32% higher LLaVA-IQA scores and at least 2x speedup compared to existing methods while maintaining robust performance across diverse scenes.

CCS Concepts

• **Computing methodologies** → Reconstruction; *Generative and developmental approaches*; *Graphics systems and interfaces*.

Keywords

Diffusion Model, 3D Reconstruction, Gaussian Splatting, Novel View Synthesis, Generative Model

ACM Reference Format:

Junlin Hao, Peiheng Wang, Haoyang Wang, Xinggong Zhang, and Zongming Guo. 2025. GaussVideoDreamer: 3D Scene Generation with Video Diffusion and Inconsistency-Aware Gaussian Splatting. In *Proceedings of Proceedings of the 33rd ACM International Conference on Multimedia (ACM MM '25)*. ACM, New York, NY, USA, 10 pages. <https://doi.org/XXXXXXX.XXXXXXX>

1 Introduction

3D scene reconstruction has long been a fundamental problem in computer vision and graphics, with significant application potential in virtual reality, autonomous driving, and robotics. Traditional 3D reconstruction algorithms [21, 28, 44, 45, 55] require dense multiview images or specialized equipment to capture scene information like RGB-D data. However, in most practical scenarios, only limited or even just a single image is available. This poses a challenging and ill-posed problem for achieving high-quality 3D reconstruction under constrained data conditions.

With the rapid development of large pre-trained models such as Large Diffusion Models (LDM) [33, 39, 42], this long-standing challenge has been primarily tackled via two generative paradigms. A large number of works [5, 12, 43, 50, 68] propose **multiview generative models**, which incorporate 3D consistency constraints within the model and train the model on 3D consistent data [26, 38] to learn generalized 3D reasoning capabilities. These methods can obtain novel view images or 3D representations in a single process, eliminating the need for iterative scene optimization. Meanwhile, another line of research [46, 53, 60, 66] focuses on leveraging diffusion models for **3D scene inpainting and completion**, where the model iteratively generates novel view information to refine and inpaint the missing regions in the scene. These works explicitly decouple 3D consistency constraints from the diffusion model by introducing an external 3D field, and this field provides geometric supervision to the diffusion process while the diffusion model reciprocally completes the 3D scene through iterative optimization.

Although remarkable progress has been achieved, current approaches still face several domain-specific challenges that hinder their practical applications.

In the context of multiview generative models, two primary weaknesses persist: **(1) Limited generalization capability**: While

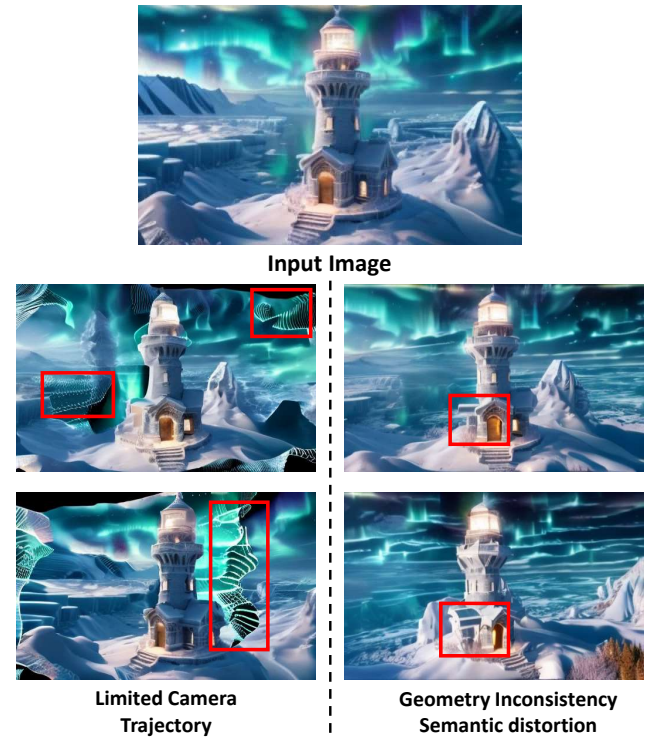


Figure 2: Multiview generative models exhibit limited generalization capability, manifesting as geometric inconsistencies and semantic distortions in synthesized views.

large generative models acquire powerful priors through extensive training, existing multiview generative methods exhibit poor performance on out-of-distribution data [12] due to scarce 3D-consistent datasets and inefficient 3D-to-2D encoding mechanisms. **(2) Information-scarce degradation**: Under limited visual information conditions, particularly during large viewpoint variations, multiview generative models exhibit quality degradation in occluded regions, resulting in fractured geometry and semantic distortions. This reveals their limited generalization capability and inherent dependency on adequate input cues, shown in Fig.2.

When shifting focus to 3D scene inpainting and completion methods, distinct weaknesses emerge: **(1) Single-view conditioning bias**: Most existing works [46, 66] employ image diffusion models that condition scene context solely on individual viewpoints and are unaware of other novel views. This inherently causes inconsistent generation across different views, compromising scene quality and increasing required optimization iterations. **(2) Crude inconsistency handling**: Existing methods employ oversimplified inconsistency processing, typically using either occlusion detection from depth [53] or 3D field smoothness [46, 60]. They fail to comprehensively analyze visual inconsistencies across images, which leads to substantial information underutilization. As a result of these constraints, the optimization process suffers from **severely slow convergence**, needing multiple hours to refine just one scene.

To address the aforementioned limitations in existing works, we pursue the technical trajectory of 3D scene inpainting and completion methods and propose GaussVideoDreamer (Fig. 3). Our key insight is that (1) video diffusion models inherently leverage richer scene context through temporal coherence, and (2) regions with higher reconstruction loss indicate geometric inconsistency, serving as effective inpainting guidance. While integrating video diffusion provides valuable temporal coherence priors, its direct application faces challenges, such as the inherent lack of 3D geometric awareness, which causes distortion and inconsistency in synthesized novel views. To solve these challenges, our method combines three key components: First, a geometry-aware initialization protocol establishes a robust coarse 3D scene to promote both quality and efficiency. Second, Inconsistency-Aware Gaussian Splatting (IAGS) jointly optimizes scene representation with a learnable error predictor, which serves as a geometric consistency checker and adaptively guides the diffusion model’s inpainting process. Third, a progressive inpainting strategy that gradually incorporates reliable multiview evidence to enhance the video diffusion model’s generation quality. Extensive quantitative evaluations demonstrate that our approach achieves **32% quality improvement** (LLaVA-IQA) and **at least 2× faster generation speed** compared to existing methods. Concretely, our contributions are the following:

1. Temporal-to-View Coherence: Replacing image diffusion with video diffusion to harness its temporal coherence as an inductive bias for multiview consistency and holistic scene understanding.

2. Advanced Inconsistency Handling: Our Inconsistency-Aware GS jointly optimizes scene representation and a learned predictor that adaptively guides video diffusion with progressive inpainting.

3. Our single-image-to-3D pipeline outperforms existing methods on out-of-distribution data, achieving higher reconstruction quality while significantly reducing processing time, as validated by several quantitative metrics.

2 Related Works

2.1 Multiview Generative Model

Recent breakthroughs in large-scale transformer-based architectures and diffusion models [31, 33, 39, 42] have shown remarkable adaptability for novel view synthesis and 3D generation from a single image, with contemporary research pursuing three principal methodological strands. The first line of research [12, 20, 24, 25, 30, 43, 52] enhances image diffusion models with explicit 3D awareness to be novel view generators, as exemplified by Zero-1-to-3 [24], which develops camera pose conditioning trained on synthetic datasets, and SyncDreamer [25] which achieves synchronized multiview consistent generation through learnable 3D geometric constraints. Alternative approaches [5, 8, 19, 49, 50, 58, 70] focus on end-to-end 3D representation learning and generation, demonstrated by LRM’s [19] pioneer transformer-based triplane-NeRF [4] generation from single images and PixelSplat’s [5] innovation through per-pixel Gaussian Splat parameter prediction. Concurrently, a third emerging paradigm [14, 16, 23, 48, 57, 59, 68] adapts video diffusion architectures to utilize inter-frame consistency with additional conditions like RGB [2, 29, 61, 63, 68], depth [11, 62], and semantic maps [32], where MotionCtrl [57] achieves viewpoint control via camera extrinsic conditioning, and ViewCrafter [68]

leverages explicit pointcloud-render inpainting for precise camera control in video generation. Although enabling efficient generation in a single process, these approaches face persistent challenges, including scarcity in 3D consistent training data and information degradation in 3D-to-2D encoding [26, 50], which harms their generalization capabilities [12] and demands prohibitive computational costs during large model training.

2.2 3D Scene Inpainting and Completion

The advent of DreamFusion [34] established another predominant 3D generation paradigm, introducing Score Distillation Sampling (SDS) to leverage 2D diffusion priors and optimize 3D scenes iteratively through single-step sampling from noisy images rendered at various viewpoints. Subsequent advances [10, 13, 27, 51] have demonstrated remarkable success in object-level reconstruction. Recent efforts [6, 9, 54, 56, 60, 66, 67, 69] have extended this framework to scene-level inpainting, though the increased complexity introduces significant challenges. Unlike object-centric cases, scene reconstruction requires handling extensive content with strict geometric coherence, leading most methods to adopt a coarse-to-refine strategy: first constructing a coarse 3D representation with depth estimation [1, 64], then completing it via diffusion guidance and inpainting loss. However, two fundamental limitations persist: image-guided diffusion models inherently lack holistic scene understanding, resulting in view-inconsistent inpainting, and the absence of explicit inconsistency detection mechanisms [41] forces SDS to inefficiently address geometric errors, resulting in unstable optimization, manifesting as blur artifacts and excessive compute demands.

3 Preliminary

Notation Convention. We maintain distinct notations for diffusion and Gaussian Splats optimization processes throughout our formulations. All superscript (t) denote GS iterations, while subscript t indicates diffusion timesteps.

3.1 Distractor-Free 3D Gaussian Splatting

We build our pipeline and technique on top of 3D Gaussian Splatting (3DGS) [21], a competitive alternative to NeRF [28], with real-time rendering speeds and memory-efficient training. It represents the 3D scene as collections of anisotropic 3D Gaussians (splats) \mathcal{G} . Each splat’s geometry is represented by a mean $\mu \in \mathbb{R}^3$, scale vector $s \in \mathbb{R}^3$, and quaternion $q \in \mathbb{R}^4$, so that the covariance, i.e. the shape of the splat is given by $\Sigma = RSS^T R^T$, where $S = \text{Diag}(s)$ and R is the rotation matrix computed from q . Each splat also has a corresponding opacity $\sigma \in \mathbb{R}$ and color $c \in \mathbb{R}^3$.

Given posed images $\{I_i\}_{i=1}^N$, $I_i \in \mathbb{R}^{H \times W}$, 3DGS optimizes these splats through volumetric rendering. Once splat positions and covariances in screen spaces are computed, the pixel color $C(\mathbf{p})$ at coordinate \mathbf{p} is computed via alpha-blending:

$$C(\mathbf{p}) = \sum_{i \in \mathcal{N}} \alpha_i c_i \prod_{j=1}^{i-1} (1 - \alpha_j), \quad \alpha_i = \sigma_i e^{-\frac{1}{2}(\mathbf{p} - \mu_i)^T \Sigma^{-1} (\mathbf{p} - \mu_i)},$$

where \mathcal{N} denotes splats overlapping \mathbf{p} , and α_i implements a Gaussian-weighted opacity. While 3DGS excels with multi-view

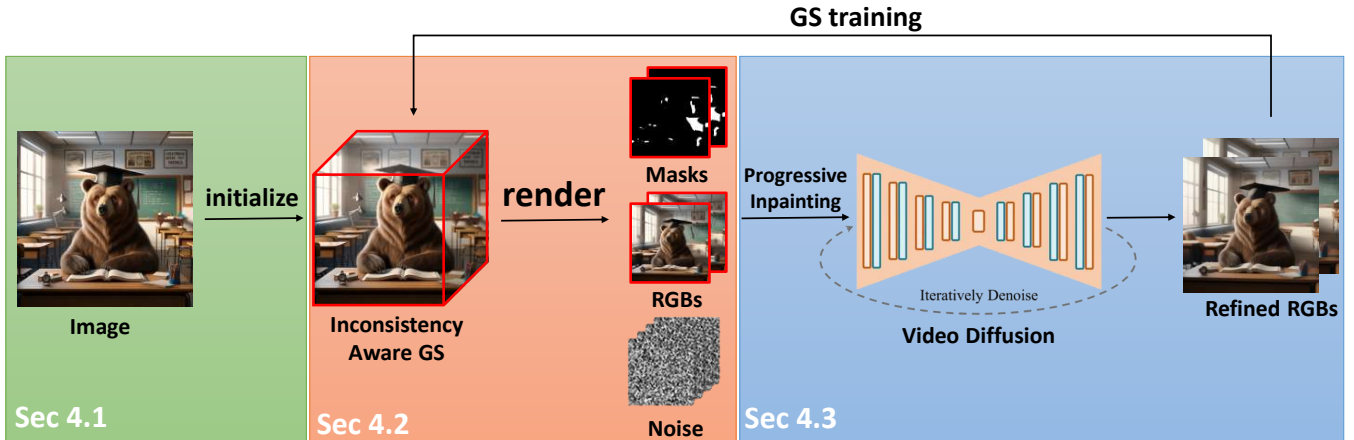


Figure 3: Overview of our pipeline. Our method first initializes a coarse video and inconsistency-aware GS (IA-GS) from a single input image (Sec. 4.1). At periodic optimization intervals, we render all viewpoint images and their corresponding inconsistency prediction masks from the IA-GS representation (Sec. 4.2). These masks and rendered images then guide a video diffusion model to perform progressive inpainting, editing regions based on their inconsistency levels (Sec. 4.3). The refined video sequence subsequently optimizes our IA-GS module and gradually generates better novel view images.

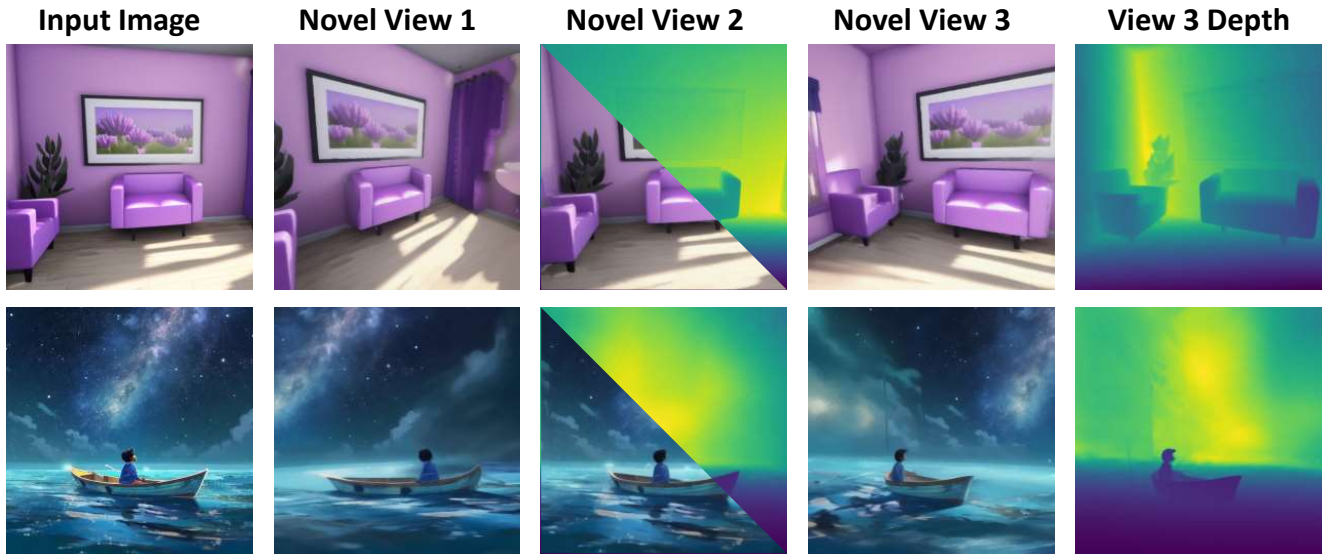


Figure 4: Qualitative Results. Left: Input reference image. Middle: Novel view renderings and RGB-depth split from our 3DGS. Right: Depth map visualization. The results demonstrate that our method can generate coherent color and consistent geometry across both indoor and outdoor scenes.

inputs, its performance degrades for single-image reconstruction due to initialization ambiguity and viewpoint overfitting. We circumvent this by initializing a coarse 3D scene from the input image and progressively refining it through novel view inpainting.

Several works [35, 40] have investigated 3DGS training on unconstrained, in-the-wild photo collections, relaxing the conventional assumption that the input images depict a perfectly consistent static 3D world. These methods identify regions violating geometric consistency as distractors — a concept analogous to the inconsistency

artifacts in our generated views. Specifically, they jointly optimize a neural network θ to predict inlier/outlier masks $\{M_j\}_{j=1}^N$ for each training image through self-supervision, optimizing the splats via a masked L1 loss:

$$\arg \min_{\mathcal{G}} \sum_{n=1}^N M_n^{(t)} \odot \|I_n - \hat{I}_n^{(t)}\|_1,$$

where the superscript (t) indexes the training iteration of \mathcal{G} and \odot denotes the Hadamard product. Building upon this framework, we adapt their distractor prediction mechanism to serve as a learnable inconsistency checker in our pipeline, enhancing its capability to identify errors and artifacts during novel view inpainting.

3.2 Conditional Video Diffusion Model

Diffusion models [17, 47] are generative models that learn to progressively denoise samples from a Gaussian distribution $x_T \sim \mathcal{N}(0, I)$, demonstrating remarkable generation capabilities across various domains. They consist of two primary components, a forward process q that gradually adds noise to clean data $x_0 \sim q_0(x_0)$ through discrete timesteps t , and a learned reverse process p_θ where a neural network $\epsilon_\theta(x_t, t)$ predicts and removes the noise at each step.

When extended to conditional generation, the model accepts additional inputs \mathbf{c} (e.g., text prompts or images) that modulate the data distribution as a conditional denoiser $\epsilon_\theta(x_t, t, \mathbf{c})$. To enhance conditional fidelity, classifier-free guidance [18] is often adapted to interpolate between conditional and unconditional predictions:

$$\tilde{\epsilon}_\theta(x_t, t, \mathbf{c}) = (1 + w)\epsilon_\theta(x_t, t, \mathbf{c}) - w\epsilon_\theta(x_t, t)$$

For video generation, the video data $x \in \mathbb{R}^{L \times 3 \times H \times W}$ is first encoded into a latent representation $z \in \mathbb{R}^{L \times C \times h \times w}$ through a frame-wise VAE encoder. Both diffusion processes operate on the complete temporal sequence in latent space, ensuring inter-frame consistency while maintaining computational efficiency. The decoded output is then reconstructed through the VAE decoder. In our framework, we strategically treat multiview renderings from smooth camera trajectories as temporal video frames, thereby enabling the video diffusion model to inpaint and refine novel views while preserving consistency.

4 Methods

4.1 Initializing a Coarse Scene

As no 3D awareness is applied to the video diffusion model, the initialization quality significantly influences the final output fidelity. To generate a coarse video sequence depicting occluded regions from the single-view input image under smooth novel view trajectories, we formulate this as an inpainting problem addressed through a warp-and-inpaint paradigm, as shown in Fig. 5. Specifically, we first estimate the depth map and focal length of the reference image I_{ref} using a monocular depth estimation model. This allows us to construct a point cloud \mathcal{P} aligned with the predefined reference camera pose C_{ref} . By rendering \mathcal{P} along a trajectory of F novel viewpoints $\{C_i\}_{i=1}^F$, we obtain rendered images $\{I_i\}_{i=1}^F$, corresponding depth maps $\{D_i\}_{i=1}^F$, and pixel masks $\{M_i^{pix}\}_{i=1}^F$ indicating regions without points.

However, directly using $\{M_i^{pix}\}_{i=1}^F$ for inpainting introduces perspective errors since these masks are subsets of the occluded regions of objects, which causes quality degradation in diffusion models without 3D awareness. To resolve this, we employ the occlusion volume technique [46] to construct a volume \mathcal{O} where all

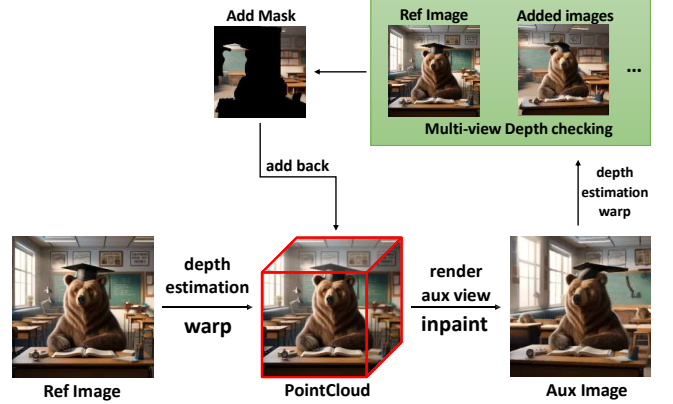


Figure 5: Overview of initialization pipeline. We first lift the input image to a point cloud \mathcal{P} , then render \mathcal{P} at auxiliary viewpoints, and inpaint the occluded regions. We warp the newly inpainted image to existing views and validate geometry through depth verification. Only geometrically consistent regions (via add mask) are added to \mathcal{P} , yielding a coarse 3D scene \mathcal{P}_{aux} that initializes both our video generation and IA-GS.

voxels occluded from C_{ref} are assumed to contain points. Rendering \mathcal{O} along $\{C_i\}_{i=1}^F$ yields occlusion depths $\{D_i\}_{i=1}^F$, from which we derive the occlusion-aware inpainting masks:

$$M_i^{occ} = M_i^{pix} \cup (D_i > \mathcal{D}_i) \quad (1)$$

To perform a high-quality initialization for the occluded regions of the scene, we choose several auxiliary viewpoints $\{C_{aux_i}\} \subset \{C_i\}_{i=1}^F$, adapting a progressive view expansion strategy that incrementally processes auxiliary viewpoints from small to large camera offsets. At each viewpoint aux_i , we utilize an image diffusion model to inpaint the occlusion regions with mask $M_{aux_i}^{occ}$ and conduct depth estimation and multi-view consistency checking through depth projection. Only pixels not occluding existing points in prior views are added to the point cloud \mathcal{P} .

Once the initial point cloud \mathcal{P}_{aux} is filled, we render the novel view images, then inpaint them using a video diffusion model with per-frame pixel masks $\{M_i^{pix}\}_{i=1}^F$ to produce a coarse but globally consistent scene video $\{I_i^{init}\}_{i=1}^F$. Crucially, we maintain separate treatment for reference-derived points versus newly added points, generating view-specific refinement masks $\{M_i^{refine}\}_{i=1}^F$ for subsequent processing.

4.2 Inconsistency Aware Gaussian Splats

We then use the coarse point cloud \mathcal{P}_{aux} to initialize our Inconsistency Aware Gaussian Splats, which develop an inconsistency detection framework tailored for 3D scene inpainting tasks. We follow existing methods to use a self-supervised MLP predictor ϕ trained with dynamically generated masks derived from the rendering loss $R_i^{(t)}$ at every training iteration (t) of Gaussian Splats \mathcal{G} . The generated mask is computed as

$$M_i^{(t)} = \mathbf{1} \left\{ \left(\mathbf{1} \left\{ R_i^{(t)} > \rho \right\} \circledast \mathbf{B} \right) > 0.5 \right\}, P \left(R_i^{(t)} > \rho \right) = \tau \quad (2)$$

where ρ denotes the generalized median threshold (percentile τ) and \mathbf{B} represents a 3×3 box filter that performs a morphological dilation via convolution (\circledast). The predictor ϕ , implemented as per-pixel 1×1 convolutions \mathcal{H} , is optimized through a bounded supervision loss that incorporates upper and lower bounds ($\mathbf{U}^{(t)}$, $\mathbf{L}^{(t)}$) computed from Eq.(2) with τ_{low} and τ_{high} respectively, and the loss $\mathcal{L}_{\text{sup}}(\phi^{(t)})$ is computed as:

$$\begin{aligned} \mathcal{L}_{\text{sup}}(\phi^{(t)}) = & \max \left(\mathbf{U}^{(t)} - \mathcal{H}(\mathbf{F}; \phi^{(t)}), 0 \right) \\ & + \max \left(\mathcal{H}(\mathbf{F}; \phi^{(t)}) - \mathbf{L}^{(t)}, 0 \right) \end{aligned} \quad (3)$$

Our approach introduces two key adaptations for 3D generation scenarios:

4.2.1 Prior-aware confidence weighting. Our framework incorporates consistency confidence priors, where geometrically warped points (e.g., from the reference view) are inherently more reliable than diffusion-generated content in occluded regions. We materialize this prior through two mechanisms: the preservation loss

$$\mathcal{L}_{\text{prior}}(\phi^{(t)}) = \max \left(M^P - \mathcal{H}(\mathbf{F}; \phi^{(t)}), 0 \right) \quad (4)$$

with $M^P = \neg M^{\text{occ}}$ protects high-confidence areas, while the discard loss

$$\mathcal{L}_{\text{discard}}(\phi^{(t)}) = - \left(M^P \circledast (1 - \mathcal{H}(\mathbf{F}; \phi^{(t)})) \circledast R_i^{(t)} \right) \quad (5)$$

actively removes the most inconsistent content. These are combined as our final loss $\mathcal{L}_{\text{mask}}(\phi^{(t)})$:

$$\begin{aligned} \mathcal{L}_{\text{mask}} = & \mathcal{L}_{\text{sup}}(\phi^{(t)}) + \lambda_{\text{prior}} \mathcal{L}_{\text{prior}}(\phi^{(t)}) \\ & + \lambda_{\text{discard}} \mathcal{L}_{\text{discard}}(\phi^{(t)}) \end{aligned} \quad (6)$$

4.2.2 Dynamic inconsistency handling. Unlike conventional 3DGS methods processing fixed image sets, our MLP predictor undergoes periodic resetting after each video refinement process to escape local optima from previous iterations. Concurrently, we progressively tighten the supervision bounds to enforce shrinking inconsistency regions as the video converges toward higher consistency. This dual strategy of predictor resetting and bound annealing ensures adaptive re-localization of emerging artifacts.

4.3 Video and Scene Refinement

Our initial coarse scene suffers from both geometric and semantic errors (e.g., lighting discontinuities) due to per-view initialization. While the inconsistency-aware mask $M^{\text{mlp}} = \text{binary}(1 - \mathcal{H}(\mathbf{F}; \phi^{(t)}))$ captures geometric errors, semantic correction relies on video diffusion. We render all views $\{\hat{I}_i^{(t)}\}_{i=1}^F$ with the current 3DGS model, encode to latents $z = \{\mathcal{E}(I_i^{(t)})\}$, then noisify to z_t at random timestep t from the diffusion model's noise schedule.

We observe that directly applying binary masks $M^{\text{mlp}} \cup M^{\text{refine}}$ to video refinement causes global inconsistencies due to the diffusion model's lack of 3D awareness, which generates distorted

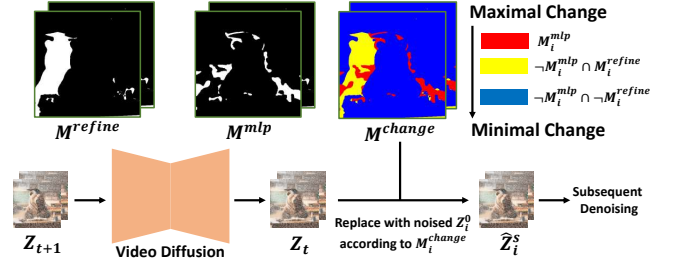


Figure 6: Overview of our video refinement method. We compute progressive change maps from inconsistency-aware masks and refinement masks to guide inpainting. We progressively integrate reliable multiview evidence for higher-quality output.

content in occluded areas that contradicts geometrically visible regions in other viewpoints. To mitigate this, we first provide richer contextual clues for occluded region by replacing binary masks with progressive change maps M^{change} , as shown in Fig. 6. We apply maximal change for geometrically inconsistent regions (M^{mlp}), mediate change for consistent generated regions ($\neg M^{\text{mlp}} \cap M^{\text{refine}}$), and minimal change for validated visible areas ($\neg M^{\text{mlp}} \cap \neg M^{\text{refine}}$). This is achieved by adjusting the inference chain length [22] - longer chains induce more modifications, allowing the diffusion model to assimilate multiview evidence from reliable regions progressively. Formally, for pixels with change weight w^{change} , we substitute the predicted latent z_t with the noised original latent z_0 on the corresponding coordinate when the current timestep t satisfies $\frac{T-t}{T} < 1 - w^{\text{change}}$. Besides, we incorporate estimated depths on current video as an additional condition to prevent excessive change in the geometric consistent regions $\neg M^{\text{mlp}}$. Then, refined latents are obtained via:

$$\hat{z} = \text{Diffusion}(z_t, M^{\text{change}}, \text{depth}, \text{text}) \quad (7)$$

The refined latents \hat{z} are decoded to $\{\tilde{I}_i\} = \mathcal{D}(\hat{z})$. We reset the MLP predictor to clear accumulated inconsistency estimates and optimize the IA-GS model using a composite loss function that balances refinement with preservation:

$$\begin{aligned} \mathcal{L}_{\text{gs}} = & \| (M^{\text{mlp}} \cup M^{\text{refine}}) \circledast (\tilde{I} - \hat{I}) \|_2^2 \\ & + \| \neg (M^{\text{mlp}} \cup M^{\text{refine}}) \circledast (I - I^{\text{init}}) \|_1 \\ & - \text{Pearson}(D, \hat{D}) \end{aligned} \quad (8)$$

where we conduct L2-driven quality improvement in refined regions, L1-based preservation of validated content, and depth correlation enforcement for 3D coherence.

5 Experiments

5.1 Experimental protocol

Datasets. Our evaluation employs 20 generated single-view images with corresponding text prompts from our baseline [46]. This synthetic dataset eliminates data acquisition biases and enables

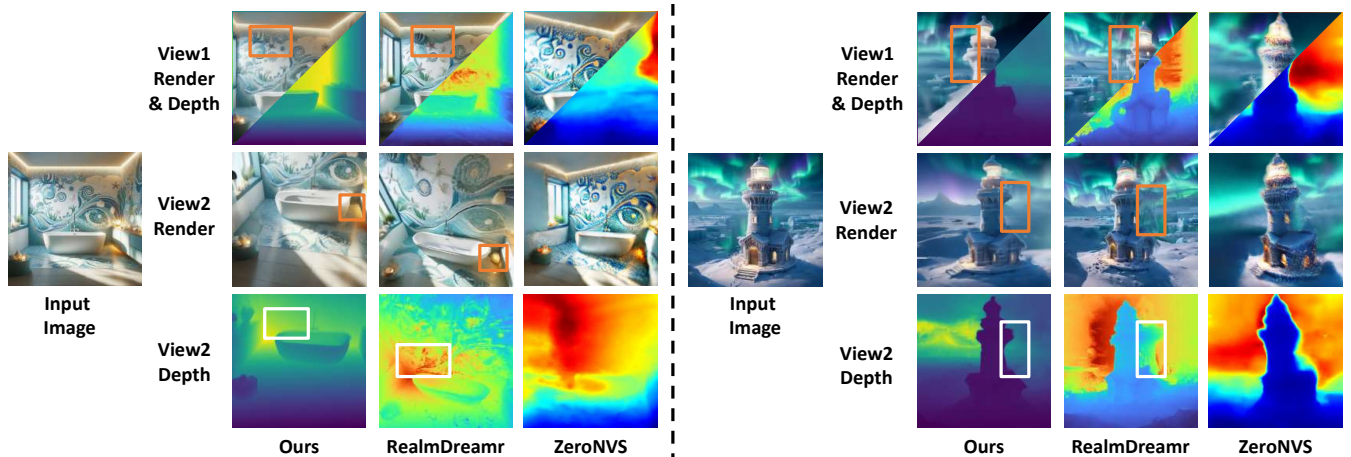


Figure 7: Qualitative Comparison. Due to our rearranged camera trajectory, the visualization is constrained to nearest-neighbor viewpoints when comparing methods. Our method generates more plausible geometry and imagery than ZeroNVS [43] and RealmDreamer [46], with significantly reduced computation time.

Table 1: Quantitative evaluations on scene renderings of our method and the baselines.

Method	CLIP \uparrow	Depth Pearson \uparrow	LLaVA-IQA Structure \uparrow	LLaVA-IQA Quality \uparrow	Train Diffusion	Time \downarrow
ZeroNVS	25.61	0.82	0.371	0.390	\checkmark	1h
RealmDreamer	31.69	0.89	0.325	0.431	\times	13 hours
Ours-Coarse	27.72	-	0.659	0.528	\times	5 min
Ours	29.52	0.97	0.763	0.572	\times	25 min

rigorous testing of generalization capabilities on novel scene compositions. For video diffusion processing, we rearrange camera trajectories to ensure smooth viewpoint transitions while maintaining physically plausible poses.

Baselines. We compare our method with concurrent 3D generation approaches based on image diffusion without embedded inconsistency awareness: ZeroNVS [43] and RealmDreamer [46]. ZeroNVS employs a fine-tuned multiview diffusion model to generate novel views conditioned on camera transformations, followed by NeRF optimization using Score Distillation Sampling (SDS) [34]. RealmDreamer progressively expands a 3D Gaussian field through iterative diffusion-based inpainting, incorporating both RGB and depth supervision.

Metrics. Since ground truth data from novel viewpoints is unavailable, conventional reconstruction metrics (e.g., PSNR, LPIPS [71]) become inapplicable for evaluation. Therefore, we adopt three complementary assessment metrics: (1) semantic alignment with text prompts measured by CLIP similarity scores [36], (2) geometric consistency quantified through Pearson correlation between rendered depth and DepthAnythingV2 [65] predicted depth, and (3) perceptual quality evaluation via LLaVA-IQA [54], where a vision-language model systematically assesses image structure and rendering quality through targeted questioning. This multi-faceted evaluation framework enables a comprehensive quantification of

both appearance preservation and geometric fidelity in the absence of ground truth references.

Implementation Details. Our pipeline’s implementation consists of the following key components: (1) The coarse stage employs PyTorch3D [37] for point cloud processing, Stable Diffusion 2.0 [39] for inpainting, and DepthPro [3] for monocular depth estimation. (2) For video diffusion, we adopt AnimateDiff [15], which integrates Temporal Transformer modules into a Stable Diffusion 1.5 backbone. (3) Depth conditioning is achieved using Video-Depth Anything [7] to predict per-frame depth maps. (4) Our 3D Gaussian Splatting (3DGS) implementation builds upon SpotLessSplat [40]. Each scene undergoes 15k training iterations, with video refinement every 2k steps. During optimization, we linearly anneal the noise level s from 0.6 to 0.3 and tighten the lower bound τ_{low} from 0.7 to 0.85. The entire process completes in 25 minutes on a single NVIDIA RTX 4090D (24GB VRAM).

5.2 Qualitative Results

Fig 4 demonstrates GaussVideoDreamer’s capability to generate high-fidelity 3D scenes with physically plausible geometry across both indoor and outdoor settings. And comparative results in Fig. 7 reveal three key advantages: (1) In bathroom scene, our method produces significantly smoother surfaces and accurately reconstructs wall patterns where RealmDreamer fails; (2) For lighthouse scene, GaussVideoDreamer correctly infers occluded regions while

RealmDreamer’s output leads to 3DGS collapse; (3) Although ZeroNVS generates plausible low-frequency structures, it struggles with blurred geometric edges and missing background elements compared to our approach.

5.3 Quantitative Metrics

Our quantitative results (Table 1) demonstrate consistent improvements across all metrics except for an acceptable CLIP score decrease, with particularly significant gains in geometric accuracy (Depth Pearson from 0.89 to 0.97) and structural integrity (LLaVA-IQA Structure from 0.325 to 0.763). Our method achieves these superior reconstruction qualities while drastically reducing computational requirements from 13 hours to just 25 minutes, concurrently improving overall LLaVA-IQA Quality from 0.431 to 0.572. These comprehensive advancements validate the effectiveness of our video diffusion framework combined with inconsistency-aware Gaussian splatting for high-fidelity 3D scene reconstruction.

Table 2: Ablation Study Results

Method	CLIP	Depth Pearson	LLaVA-IQA Structure	LLaVA-IQA Quality
w/o Init	28.82	0.94	0.282	0.164
w/o IA-GS	30.08	0.96	0.671	0.515
Ours	29.52	0.97	0.763	0.572

5.4 Ablations

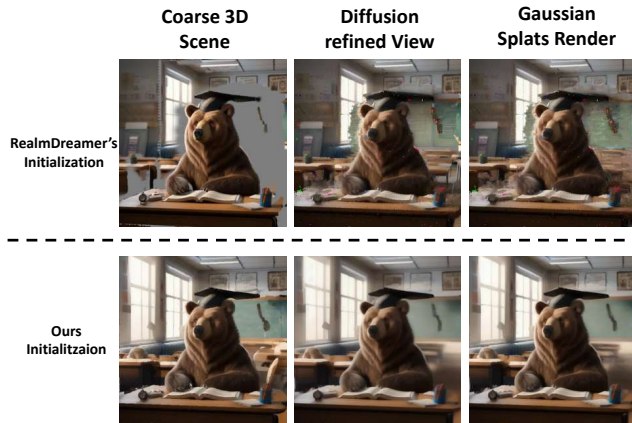


Figure 8: Compared to RealmDreamer’s gray-splat initialization causing inconsistent generation and 3DGS failures, our occlusion-aware inpainting enables more stable 3D/video diffusion refinement.

We conduct an ablation study to validate two critical designs: our coarse video initialization strategy and Inconsistency-Aware GS. First, when replacing our initialization with RealmDreamer’s approach, which depends solely on video diffusion to hallucinate

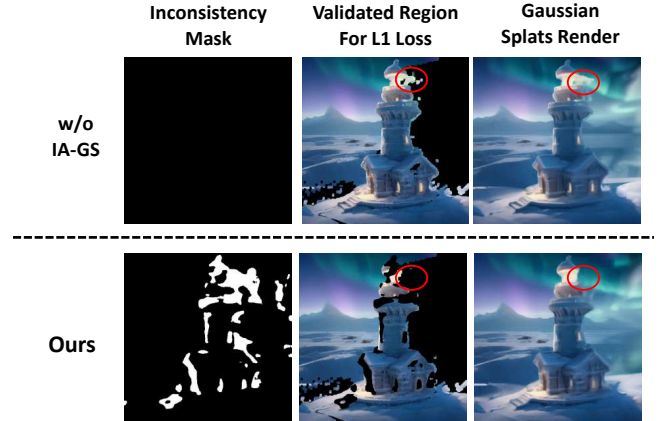


Figure 9: Ablation Results on Inconsistency-Aware GS. Our IA-GS module identifies and rectifies erroneously projected regions through targeted diffusion-based erasure, significantly enhancing 3D reconstruction quality.

occluded regions without initialized inpainting and warping. The absence of 3D consistency constraints in the video diffusion leads to severe distortions in occluded areas, ultimately causing catastrophic failure in 3DGS optimization (Fig. 8). Second, ablation of our IA-GS (reverting to vanilla 3DGS) results in persistent floating artifacts due to undetected erroneous projections from the coarse stage (Fig. 9). Quantitative results (Table 2) reveal that our initialization improves all key metrics and IA-GS achieves superior scene integrity with a marginal CLIP score reduction. These comparisons demonstrate that both proposed components are indispensable for achieving geometrically stable and high-quality synthesis when integrating video diffusion into 3D generation pipelines.

6 Conclusion and Limitation

Conclusion. We present GaussVideoDreamer, a novel pipeline for single-image 3D generation that harnesses video diffusion while addressing its consistency limitations. Our framework first establishes a geometrically stable coarse reconstruction through iterative view inpainting, then introduces Inconsistency-Aware Gaussian Splatting to dynamically detect 3D errors, and utilizes video diffusion to refine the scene with its temporal-to-view coherence adaptation. Without the requirement to fine-tune the diffusion model, our method outperforms existing approaches in both quality and efficiency, as validated by multiple qualitative results and quantitative metrics.

Limitation. Our generation quality is primarily limited by the video diffusion prior (AnimateDiff), which was adapted from an image diffusion model lacking dedicated video inpainting training [15]. Its limited video generation capability manifests as frame inconsistencies in longer sequences, progressive color shifts, and high-frequency detail degradation. Our pipeline consequently depends on high-quality initialization and constrained refinement iterations to ensure optimization stability – a limitation that could

be addressed through improved video diffusion architectures in future work.

References

- [1] Shariq Farooq Bhat, Reiner Birkel, Diana Wofk, Peter Wonka, and Matthias Müller. 2023. ZoeDepth: Zero-shot Transfer by Combining Relative and Metric Depth. arXiv:2302.12288 [cs.CV] <https://arxiv.org/abs/2302.12288>
- [2] Andreas Blattmann, Tim Dockhorn, Sumith Kulal, Daniel Mendelevitch, Maciej Kilian, Dominik Lorenz, Yam Levi, Zion English, Vikram Voleti, Adam Letts, Varun Jampani, and Robin Rombach. 2023. Stable Video Diffusion: Scaling Latent Video Diffusion Models to Large Datasets. arXiv:2311.15127 [cs.CV] <https://arxiv.org/abs/2311.15127>
- [3] Aleksei Bochkovskii, Amaël Delaunoy, Hugo Germain, Marcel Santos, Yichao Zhou, Stephan R. Richter, and Vladlen Koltun. 2024. Depth Pro: Sharp Monocular Metric Depth in Less Than a Second. arXiv:2410.02073 [cs.CV] <https://arxiv.org/abs/2410.02073>
- [4] Eric R. Chan, Connor Z. Lin, Matthew A. Chan, Koki Nagano, Boxiao Pan, Shalini De Mello, Orazio Gallo, Leonidas Guibas, Jonathan Tremblay, Sameh Khamis, Tero Karras, and Gordon Wetzstein. 2022. Efficient Geometry-aware 3D Generative Adversarial Networks. arXiv:2112.07945 [cs.CV] <https://arxiv.org/abs/2112.07945>
- [5] David Charatan, Sizhe Li, Andrea Tagliasacchi, and Vincent Sitzmann. 2024. pixelsplat: 3D Gaussian Splats from Image Pairs for Scalable Generalizable 3D Reconstruction. arXiv:2312.12337 [cs.CV] <https://arxiv.org/abs/2312.12337>
- [6] Luxi Chen, Zihan Zhou, Min Zhao, Yikai Wang, Ge Zhang, Wenhao Huang, Hao Sun, Ji-Rong Wen, and Chongxuan Li. 2025. FlexWorld: Progressively Expanding 3D Scenes for Flexible-View Synthesis. arXiv:2503.13265 [cs.CV] <https://arxiv.org/abs/2503.13265>
- [7] Sili Chen, Hengkai Guo, Shengnan Zhu, Feihu Zhang, Zilong Huang, Jiashi Feng, and Bingyi Kang. 2025. Video Depth Anything: Consistent Depth Estimation for Super-Long Videos. arXiv:2501.12375 [cs.CV] <https://arxiv.org/abs/2501.12375>
- [8] Yuedong Chen, Haofei Xu, Chuanxia Zheng, Bohan Zhuang, Marc Pollefeys, Andreas Geiger, Tat-Jen Cham, and Jianfei Cai. 2024. *MVSplat: Efficient 3D Gaussian Splatting from Sparse Multi-view Images*. Springer Nature Switzerland, 370–386. doi:10.1007/978-3-031-72664-4_21
- [9] Jaeyoung Chung, Suyoung Lee, Hyeonjin Nam, Jaerin Lee, and Kyoung Mu Lee. 2023. LucidDreamer: Domain-free Generation of 3D Gaussian Splatting Scenes. arXiv preprint arXiv:2311.13384 (2023).
- [10] Congyue Deng, Chiyu Max Jiang, C. Qi, Xinchun Yan, Yin Zhou, Leonidas J. Guibas, and Drago Anguelov. 2022. NeRDi: Single-View NeRF Synthesis with Language-Guided Diffusion as General Image Priors. 2023 *IEEE/CVF Conference on Computer Vision and Pattern Recognition (CVPR)* (2022), 20637–20647. <https://api.semanticscholar.org/CorpusID:254366717>
- [11] Patrick Esser, Johnathan Chiu, Parmida Atighehchian, Jonathan Granskog, and Anastasis Germanidis. 2023. Structure and Content-Guided Video Synthesis with Diffusion Models. arXiv:2302.03011 [cs.CV] <https://arxiv.org/abs/2302.03011>
- [12] Ruiqi Gao*, Aleksander Holynski*, Philipp Henzler, Arthur Brussee, Ricardo Martin-Brualla, Pratul P. Srinivasan, Jonathan T. Barron, and Ben Poole*. 2024. CAT3D: Create Anything in 3D with Multi-View Diffusion Models. *Advances in Neural Information Processing Systems* (2024).
- [13] Jiatao Gu, Alex Trevithick, Kai-En Lin, Joshua M. Susskind, Christian Theobalt, Lingjie Liu, and Ravi Ramamoorthi. 2023. NerfDiff: Single-image View Synthesis with NeRF-guided Distillation from 3D-aware Diffusion. In *International Conference on Machine Learning*. <https://api.semanticscholar.org/CorpusID:257039008>
- [14] Yuwei Guo, Ceyuan Yang, Anyi Rao, Maneesh Agrawala, Dahua Lin, and Bo Dai. 2023. SparseCtrl: Adding Sparse Controls to Text-to-Video Diffusion Models. arXiv:2311.16933 [cs.CV]
- [15] Yuwei Guo, Ceyuan Yang, Anyi Rao, Zhengyang Liang, Yaohui Wang, Yu Qiao, Maneesh Agrawala, Dahua Lin, and Bo Dai. 2024. AnimateDiff: Animate Your Personalized Text-to-Image Diffusion Models without Specific Tuning. arXiv:2307.04725 [cs.CV] <https://arxiv.org/abs/2307.04725>
- [16] Hao He, Yinghao Xu, Yuwei Guo, Gordon Wetzstein, Bo Dai, Hongsheng Li, and Ceyuan Yang. 2024. CameraCtrl: Enabling Camera Control for Text-to-Video Generation. arXiv:2404.02101 [cs.CV]
- [17] Jonathan Ho, Ajay Jain, and Pieter Abbeel. 2020. Denoising Diffusion Probabilistic Models. arXiv:2006.11239 [cs.LG] <https://arxiv.org/abs/2006.11239>
- [18] Jonathan Ho and Tim Salimans. 2022. Classifier-Free Diffusion Guidance. arXiv:2207.12598 [cs.LG] <https://arxiv.org/abs/2207.12598>
- [19] Yicong Hong, Kai Zhang, Jiuxiang Gu, Sai Bi, Yang Zhou, Difan Liu, Feng Liu, Kalyan Sunkavalli, Trung Bui, and Hao Tan. 2024. LRM: Large Reconstruction Model for Single Image to 3D. arXiv:2311.04400 [cs.CV] <https://arxiv.org/abs/2311.04400>
- [20] Hanzhe Hu, Zhizhuo Zhou, Varun Jampani, and Shubham Tulsiani. 2024. MVD-Fusion: Single-view 3D via Depth-consistent Multi-view Generation. arXiv:2404.03656 [cs.CV] <https://arxiv.org/abs/2404.03656>
- [21] Bernhard Kerbl, Georgios Kopanas, Thomas Leimkühler, and George Drettakis. 2023. 3D Gaussian Splatting for Real-Time Radiance Field Rendering. *ACM Transactions on Graphics* 42, 4 (July 2023). <https://repo-sam.inria.fr/fungraph/3d-gaussian-splatting/>
- [22] Eran Levin and Ohad Fried. 2023. Differential Diffusion: Giving Each Pixel Its Strength. arXiv:2306.00950 [cs.CV]
- [23] Fangfu Liu, Wenqiang Sun, Hanyang Wang, Yikai Wang, Haowen Sun, Junliang Ye, Jun Zhang, and Yueqi Duan. 2024. ReconX: Reconstruct Any Scene from Sparse Views with Video Diffusion Model. arXiv:2408.16767 [cs.CV] <https://arxiv.org/abs/2408.16767>
- [24] Ruoshi Liu, Rundi Wu, Basile Van Hoorick, Pavel Tokmakov, Sergey Zakharov, and Carl Vondrick. 2023. Zero-1-to-3: Zero-shot One Image to 3D Object. arXiv:2303.11328 [cs.CV]
- [25] Yuan Liu, Cheng Lin, Zijiao Zeng, Xiaoxiao Long, Lingjie Liu, Taku Komura, and Wenping Wang. 2023. SyncDreamer: Generating Multiview-consistent Images from a Single-view Image. arXiv preprint arXiv:2309.03453 (2023).
- [26] Baorui Ma, Huachen Gao, Haoge Deng, Zhengxiang Luo, Tiejun Huang, Lulu Tang, and Xinlong Wang. 2025. You See it, You Got it: Learning 3D Creation on Pose-Free Videos at Scale. arXiv:2412.06699 [cs.CV] <https://arxiv.org/abs/2412.06699>
- [27] Luke Melas-Kyriazi, Christian Rupprecht, Iro Laina, and Andrea Vedaldi. 2023. RealFusion: 360 deg Reconstruction of Any Object from a Single Image. arXiv:2302.10663 [cs.CV] <https://arxiv.org/abs/2302.10663>
- [28] Ben Mildenhall, Pratul P. Srinivasan, Matthew Tanicli, Jonathan T. Barron, Ravi Ramamoorthi, and Ren Ng. 2020. NeRF: Representing Scenes as Neural Radiance Fields for View Synthesis. In *ECCV*.
- [29] Norman Müller, Katja Schwarz, Barbara Roessle, Lorenzo Porzi, Samuel Rota Bulò, Matthias Nießner, and Peter Kotschieder. 2024. MultiDiff: Consistent Novel View Synthesis from a Single Image. arXiv:2406.18524 [cs.CV] <https://arxiv.org/abs/2406.18524>
- [30] Thang-Anh-Quan Nguyen, Nathan Piasco, Luis Roldão, Moussab Bennehar, Dzmitry V. Tsishkou, Laurent Caraffa, Jean-Philippe Tarel, and Roland Br' emond. 2025. Pointmap-Conditioned Diffusion for Consistent Novel View Synthesis. *ArXiv abs/2501.02913* (2025). <https://api.semanticscholar.org/CorpusID:275336608>
- [31] William Peebles and Saining Xie. 2023. Scalable Diffusion Models with Transformers. arXiv:2212.09748 [cs.CV] <https://arxiv.org/abs/2212.09748>
- [32] Elia Peruzzo, Vidit Goel, DeJia Xu, Xingqian Xu, Yifan Jiang, Zhangyang Wang, Humphrey Shi, and Nicu Sebe. 2024. VASE: Object-Centric Appearance and Shape Manipulation of Real Videos. arXiv:2401.02473 [cs.CV] <https://arxiv.org/abs/2401.02473>
- [33] Dustin Podell, Zion English, Kyle Lacey, Andreas Blattmann, Tim Dockhorn, Jonas Müller, Joe Penna, and Robin Rombach. 2023. Sdxl: Improving latent diffusion models for high-resolution image synthesis. arXiv preprint arXiv:2307.01952 (2023).
- [34] Ben Poole, Ajay Jain, Jonathan T. Barron, and Ben Mildenhall. 2022. DreamFusion: Text-to-3D using 2D Diffusion. arXiv:2209.14988 [cs.CV] <https://arxiv.org/abs/2209.14988>
- [35] Vadim Pryadilshchikov, Alexander Markin, Artem Komarichev, Ruslan Rakhimov, Peter Wonka, and Evgeny Burnaev. 2024. T-3DGS: Removing Transient Objects for 3D Scene Reconstruction. *ArXiv abs/2412.00155* (2024). <https://api.semanticscholar.org/CorpusID:274436034>
- [36] Alec Radford, Jong Wook Kim, Chris Hallacy, Aditya Ramesh, Gabriel Goh, Sandhini Agarwal, Girish Sastry, Amanda Askell, Pamela Mishkin, Jack Clark, Gretchen Krueger, and Ilya Sutskever. 2021. Learning Transferable Visual Models From Natural Language Supervision. arXiv:2103.00020 [cs.CV] <https://arxiv.org/abs/2103.00020>
- [37] Nikhila Ravi, Jeremy Reizenstein, David Novotny, Taylor Gordon, Wan-Yen Lo, Justin Johnson, and Georgia Gkioxari. 2020. Accelerating 3D Deep Learning with PyTorch3D. arXiv:2007.08501 [cs.CV] <https://arxiv.org/abs/2007.08501>
- [38] Jeremy Reizenstein, Roman Shapovalov, Philipp Henzler, Luca Sbordone, Patrick Labatut, and David Novotny. 2021. Common Objects in 3D: Large-Scale Learning and Evaluation of Real-life 3D Category Reconstruction. arXiv:2109.00512 [cs.CV] <https://arxiv.org/abs/2109.00512>
- [39] Robin Rombach, Andreas Blattmann, Dominik Lorenz, Patrick Esser, and Björn Ommer. 2022. High-resolution image synthesis with latent diffusion models. In *Proceedings of the IEEE/CVF conference on computer vision and pattern recognition*. 10684–10695.
- [40] Sara Sabour, Lily Goli, George Kopanas, Mark Matthews, Dmitry Lagun, Leonidas Guibas, Alec Jacobson, David J. Fleet, and Andrea Tagliasacchi. 2024. SpotLessS-plats: Ignoring Distractors in 3D Gaussian Splatting. arXiv:2406.20055 (2024).
- [41] Sara Sabour, Suhani Vora, Daniel Duckworth, Ivan Krasin, David J. Fleet, and Andrea Tagliasacchi. 2024. RobustNeRF: Ignoring Distractors with Robust Losses. arXiv:2302.00833 [cs.CV] <https://arxiv.org/abs/2302.00833>
- [42] Chitwan Saharia, William Chan, Saurabh Saxena, Lala Li, Jay Whang, Emily L. Denton, Kamyar Ghasemipour, Raphael Gontijo Lopes, Burcu Karagol Ayan, Tim Salimans, et al. 2022. Photorealistic text-to-image diffusion models with deep language understanding. *Advances in neural information processing systems* 35

- (2022), 36479–36494.
- [43] Kyle Sargent, Zizhang Li, Tanmay Shah, Charles Herrmann, Hong-Xing Yu, Yunzhi Zhang, Eric Ryan Chan, Dmitry Lagun, Li Fei-Fei, Deqing Sun, and Jiajun Wu. 2023. ZeroNVS: Zero-Shot 360-Degree View Synthesis from a Single Real Image. *CVPR, 2024* (2023).
- [44] Johannes Lutz Schönberger and Jan-Michael Frahm. 2016. Structure-from-Motion Revisited. In *Conference on Computer Vision and Pattern Recognition (CVPR)*.
- [45] Johannes Lutz Schönberger, Enliang Zheng, Marc Pollefeys, and Jan-Michael Frahm. 2016. Pixelwise View Selection for Unstructured Multi-View Stereo. In *European Conference on Computer Vision (ECCV)*.
- [46] Jaidev Shriram, Alex Trevithick, Lingjie Liu, and Ravi Ramamoorthi. 2025. Realm-Dreamer: Text-Driven 3D Scene Generation with Inpainting and Depth Diffusion. *International Conference on 3D Vision (3DV)*.
- [47] Jiaming Song, Chenlin Meng, and Stefano Ermon. 2022. Denoising Diffusion Implicit Models. arXiv:2010.02502 [cs.LG] <https://arxiv.org/abs/2010.02502>
- [48] Wenqiang Sun, Shuo Chen, Fangfu Liu, Zilong Chen, Yueqi Duan, Jun Zhang, and Yikai Wang. 2024. DimensionX: Create Any 3D and 4D Scenes from a Single Image with Controllable Video Diffusion. *arXiv preprint arXiv:2411.04928* (2024).
- [49] Stanislaw Szymanowicz, Eldar Insafutdinov, Chuanxia Zheng, Dylan Campbell, João F. Henriques, Christian Rupprecht, and Andrea Vedaldi. 2024. Flash3D: Feed-Forward Generalisable 3D Scene Reconstruction from a Single Image. arXiv:2406.04343 [cs.CV] <https://arxiv.org/abs/2406.04343>
- [50] Stanislaw Szymanowicz, Jason Y. Zhang, Pratul Srinivasan, Ruiqi Gao, Arthur Brussee, Aleksander Holynski, Ricardo Martin-Brualla, Jonathan T. Barron, and Philipp Henzler. 2025. Bolt3D: Generating 3D Scenes in Seconds. arXiv:2503.14445 [cs.CV] <https://arxiv.org/abs/2503.14445>
- [51] Junshu Tang, Tengfei Wang, Bo Zhang, Ting Zhang, Ran Yi, Lizhuang Ma, and Dong Chen. 2023. Make-It-3D: High-Fidelity 3D Creation from A Single Image with Diffusion Prior. arXiv:2303.14184 [cs.CV] <https://arxiv.org/abs/2303.14184>
- [52] Ayush Tewari, Tianwei Yin, George Cazenavette, Semon Rezchikov, Joshua B. Tenenbaum, Frédo Durand, William T. Freeman, and Vincent Sitzmann. 2023. Diffusion with Forward Models: Solving Stochastic Inverse Problems Without Direct Supervision. arXiv:2306.11719 [cs.CV] <https://arxiv.org/abs/2306.11719>
- [53] Guangcong Wang, Peng Wang, Zhaoxi Chen, Wenping Wang, Chen Change Loy, and Ziwei Liu. 2024. PERF: Panoramic Neural Radiance Field from a Single Panorama. *IEEE Transactions on Pattern Analysis and Machine Intelligence (TPAMI)* (2024).
- [54] Haiping Wang, Yuan Liu, Ziwei Liu, Wenping Wang, Zhen Dong, and Bisheng Yang. 2024. VistaDream: Sampling multiview consistent images for single-view scene reconstruction. arXiv:2410.16892 [cs.CV] <https://arxiv.org/abs/2410.16892>
- [55] Shuzhe Wang, Vincent Leroy, Johann Cabon, Boris Chidlovskii, and Jerome Revaud. 2024. DUST3R: Geometric 3D Vision Made Easy. In *CVPR*.
- [56] Zhengyi Wang, Cheng Lu, Yikai Wang, Fan Bao, Chongxuan Li, Hang Su, and Jun Zhu. 2023. ProlificDreamer: High-Fidelity and Diverse Text-to-3D Generation with Variational Score Distillation. arXiv:2305.16213 [cs.LG] <https://arxiv.org/abs/2305.16213>
- [57] Zhouxia Wang, Ziyang Yuan, Xintao Wang, Tianshui Chen, Menghan Xia, Ping Luo, and Ying Shan. 2024. MotionCtrl: A Unified and Flexible Motion Controller for Video Generation. arXiv:2312.03641 [cs.CV] <https://arxiv.org/abs/2312.03641>
- [58] Christopher Wewer, Kevin Raj, Eddy Ilg, Bernt Schiele, and Jan Eric Lenssen. 2024. latentSplat: Autoencoding Variational Gaussians for Fast Generalizable 3D Reconstruction. arXiv:2403.16292 [cs.CV] <https://arxiv.org/abs/2403.16292>
- [59] Rundi Wu, Ruiqi Gao, Ben Poole, Alex Trevithick, Changxi Zheng, Jonathan T. Barron, and Aleksander Holynski. 2024. CAT4D: Create Anything in 4D with Multi-View Video Diffusion Models. arXiv:2411.18613 [cs.CV] <https://arxiv.org/abs/2411.18613>
- [60] Rundi Wu, Ben Mildenhall, Philipp Henzler, Keunhong Park, Ruiqi Gao, Daniel Watson, Pratul P. Srinivasan, Dor Verbin, Jonathan T. Barron, Ben Poole, and Aleksander Holynski. 2023. ReconFusion: 3D Reconstruction with Diffusion Priors. *arXiv* (2023).
- [61] Jinbo Xing, Hanyuan Liu, Menghan Xia, Yong Zhang, Xintao Wang, Ying Shan, and Tien-Tsin Wong. 2024. ToonCrafter: Generative Cartoon Interpolation. arXiv:2405.17933 [cs.CV] <https://arxiv.org/abs/2405.17933>
- [62] Jinbo Xing, Menghan Xia, Yuxin Liu, Yuechen Zhang, Yong Zhang, Yingqing He, Hanyuan Liu, Haoxin Chen, Xiaodong Cun, Xintao Wang, Ying Shan, and Tien-Tsin Wong. 2023. Make-Your-Video: Customized Video Generation Using Textual and Structural Guidance. arXiv:2306.00943 [cs.CV] <https://arxiv.org/abs/2306.00943>
- [63] Jinbo Xing, Menghan Xia, Yong Zhang, Haoxin Chen, Wangbo Yu, Hanyuan Liu, Xintao Wang, Tien-Tsin Wong, and Ying Shan. 2023. DynamiCrafter: Animating Open-domain Images with Video Diffusion Priors. arXiv:2310.12190 [cs.CV] <https://arxiv.org/abs/2310.12190>
- [64] Lihe Yang, Bingyi Kang, Zilong Huang, Xiaogang Xu, Jiashi Feng, and Hengshuang Zhao. 2024. Depth Anything: Unleashing the Power of Large-Scale Unlabeled Data. In *CVPR*.
- [65] Lihe Yang, Bingyi Kang, Zilong Huang, Zhen Zhao, Xiaogang Xu, Jiashi Feng, and Hengshuang Zhao. 2024. Depth Anything V2. *arXiv:2406.09414* (2024).
- [66] Hong-Xing Yu, Haoyi Duan, Charles Herrmann, William T. Freeman, and Jiajun Wu. 2025. WonderWorld: Interactive 3D Scene Generation from a Single Image. In *CVPR*.
- [67] Hong-Xing Yu, Haoyi Duan, Junhwa Hur, Kyle Sargent, Michael Rubinstein, William T. Freeman, Forrester Cole, Deqing Sun, Noah Snavely, Jiajun Wu, and Charles Herrmann. 2024. Wonderjourney: Going from Anywhere to Everywhere. In *CVPR*.
- [68] Wangbo Yu, Jinbo Xing, Li Yuan, Wenbo Hu, Xiaoyu Li, Zhipeng Huang, Xiangjun Gao, Tien-Tsin Wong, Ying Shan, and Yonghong Tian. 2024. ViewCrafter: Taming Video Diffusion Models for High-fidelity Novel View Synthesis. *arXiv preprint arXiv:2409.02048* (2024).
- [69] Jingbo Zhang, Xiaoyu Li, Ziyu Wan, Can Wang, and Jing Liao. 2023. Text2NeRF: Text-Driven 3D Scene Generation with Neural Radiance Fields. *arXiv preprint arXiv:2305.11588* (2023).
- [70] Kai Zhang, Sai Bi, Hao Tan, Yuanbo Xiangli, Nanxuan Zhao, Kalyan Sunkavalli, and Zexiang Xu. 2024. GS-LRM: Large Reconstruction Model for 3D Gaussian Splatting. arXiv:2404.19702 [cs.CV] <https://arxiv.org/abs/2404.19702>
- [71] Richard Zhang, Phillip Isola, Alexei A. Efros, Eli Shechtman, and Oliver Wang. 2018. The Unreasonable Effectiveness of Deep Features as a Perceptual Metric. arXiv:1801.03924 [cs.CV] <https://arxiv.org/abs/1801.03924>